

Radar clutter suppression and target discrimination using twin inverted pulses

T. G. Leighton, G. H. Chua, P. R. White, K. F. Tong, H. D. Griffiths and D. J. Daniels

Proc. R. Soc. A 2013 **469**, 20130512, published 23 October 2013

Supplementary data

["Data Supplement"](#)

<http://rspa.royalsocietypublishing.org/content/suppl/2013/10/22/rspa.2013.0512.DC1.html>

References

[This article cites 16 articles, 2 of which can be accessed free](#)

<http://rspa.royalsocietypublishing.org/content/469/2160/20130512.full.html#ref-list-1>

Subject collections

Articles on similar topics can be found in the following collections

[acoustics](#) (31 articles)

[electrical engineering](#) (20 articles)

Email alerting service

Receive free email alerts when new articles cite this article - sign up in the box at the top right-hand corner of the article or click [here](#)

Research



Cite this article: Leighton TG, Chua GH, White PR, Tong KF, Griffiths HD, Daniels DJ. 2013 Radar clutter suppression and target discrimination using twin inverted pulses. *Proc R Soc A* 469: 20130512. <http://dx.doi.org/10.1098/rspa.2013.0512>

Received: 1 August 2013

Accepted: 24 September 2013

Subject Areas:

electrical engineering, acoustics

Keywords:

radar, clutter, target, nonlinear, harmonic, mobile phone

Author for correspondence:

T. G. Leighton

e-mail: tgl@soton.ac.uk

Electronic supplementary material is available at <http://dx.doi.org/10.1098/rspa.2013.0512> or via <http://rspa.royalsocietypublishing.org>.

Radar clutter suppression and target discrimination using twin inverted pulses

T. G. Leighton¹, G. H. Chua¹, P. R. White¹, K. F. Tong²,
H. D. Griffiths² and D. J. Daniels³

¹Institute of Sound and Vibration Research (ISVR), Faculty of Engineering and the Environment, University of Southampton, Highfield, Southampton SO17 1BJ, UK

²Department of Electronic and Electrical Engineering, University College London (UCL), Gower Street, London WC1E 6BT, UK

³Cobham Technical Services, Cleve Road, Leatherhead, Surrey KT22 7SA, UK

The proposition that the use of twin inverted pulses could enhance radar is tested. This twin inverted pulse radar (TWIPR) is applied to five targets. A representative target of interest (a dipole with a diode across its feedpoint) is typical of covert circuitry one might wish to detect (e.g. in devices associated with covert communications, espionage or explosives), and then distinguish from other metal ('garbage' or 'clutter'), here represented by an aluminium plate and a rusty bench clamp. In addition, two models of mobile phones are tested to see whether TWIPR can distinguish whether each is off, on or whether it contains a valid SIM card. Given that a small, inexpensive, lightweight device requiring no batteries can produce a signal that is 50 dB above clutter in this test, the options are discussed for using such technology for animal tagging or to allow the location and identification of buried personnel who opt to carry them (rescue workers, skiers in avalanche areas, miners, etc.). The results offer the possibility that buried catastrophe victims not carrying such tags might still be located by TWIPR scattering from their mobile phones, even when the phones are turned off or the batteries have no charge remaining.

1. Introduction

There is a requirement for radar to be able to distinguish true 'targets' from 'clutter' (other scattering objects which might be mistaken for a genuine target, and

so generate false alarms). An example would be in distinguishing certain types of electronic circuits that might be hidden through burial alongside metallic garbage where traditional radar and metal detectors are triggered by false targets ('clutter') to an extent that search operations become unacceptably slow. An example requirement is for radar that would detect and identify covert communications or espionage devices hidden in the walls of buildings, or within natural objects (e.g. stones, trees) or electronic equipment present in locations (caves, woodland, garments, rubble or snow) where its presence indicates potentially hostile human activity or catastrophe victims in need of rescue. One feature that may be used to distinguish between clutter and a target is based on nonlinearity. For instance, many electronic components can scatter radar signals nonlinearly if driven by a sufficiently strong radar signal, in contrast to naturally occurring objects which tend to scatter linearly.

Recently, advances in distinguishing targets from clutter, using the linear/nonlinear scattering from each, were introduced into sonar and those papers proposed that the same technique would work with radar [1,2]. This paper experimentally tests that proposal. The technique uses a signal consisting of two pulses in quick succession, one identical to the other but phase inverted, to distinguish nonlinear scatterers from linearly scattering objects [3]. This was shown to be effective at enhancing active sonar at sea, where the clutter was provided by the bubbles in the wakes of a ferry and a commercial ship [4,5]. This twin inverted pulse sonar (TWIPS) was particularly effective at distinguishing targets from bubble clutter and served a secondary purpose in enhancing target detection (reducing, for example, the rate of false alarms, even one of which can disrupt operations, ship movements, etc.). TWIPS was then generalized into biased pulse summation sonar (BiaPSS) which performs similarly but which uses signals that are simpler for power amplifiers and transducers to generate [6,7].

The authors proposed that the TWIPS method could be applied to electromagnetic waves, and this paper investigates a new form of radar, twin inverted pulse radar (TWIPR; [1,2,4,5]). As with TWIPS, the method distinguishes linear scatterers from nonlinear ones. TWIPR might therefore distinguish soil and vegetation (which scatter radar linearly) from semiconductors (which generate odd and even harmonics when scattering radar pulses). Moreover, these scatterers could also be discriminated from rusty metal, which predominantly generates odd harmonics. Such scattering degrades the performance of radar domes (radomes) through the clutter it produces, known as the 'rusty bolt' effect [8]. In addition to the applications discussed above, such schemes could be extended to other radiations, such as magnetic resonance imaging (MRI) and light detection and ranging (LIDAR), which, for example, scatters nonlinearly from combustion products, offering the possibility of early fire detection systems [1,2]. There is an important distinction between the use of twin inverted pulse methods for sonar and radar. In the scenarios for which TWIPS was designed, the clutter scatters nonlinearly and the target linearly. In the radar problem addressed here, these properties are reversed (as they are with medical contrast agents; [9]).

Nonlinear scattering by targets is already used in harmonic radar which exploits the rectifying properties of different types of junctions to detect the re-radiated harmonics from an illuminated target [10]. The two most common junctions are the metal-to-metal junction and the semiconductor junction. The latter is found in the electronic devices and while it can be exploited for the detection of concealed electronic devices, it has been intentionally optimized as a tracking transponder. Such use of a diode coupled to a high-gain antenna (a semiconductor junction) has been reported in locating avalanche victims, and as tags for insect and animal tracking [11–13]. When an object with nonlinear impedance is illuminated by an electromagnetic signal, the rectification properties of the nonlinear impedances cause new signal components to be generated at frequencies that are exact multiples of the frequency of the incident waveform. These new components are radiated and can be detected with receivers used in conventional radar. Metal-to-metal interfaces form junctions that exhibit nonlinear voltage-current characteristics that are symmetric with respect to the sign of the voltage and current. Semiconductor junctions have asymmetric current and voltage characteristics. They respond differently to a positive applied voltage than to a negative applied voltage. The corresponding

nonlinear responses from these two types of junction cause the metal-to-metal junctions to generate predominantly odd harmonics [14,15], and the semiconductor junctions to generate both odd and even harmonics [10].

A limited number of tactical radar units were developed to exploit these nonlinear phenomena. One of the earliest is the metal target re-radiation system developed for the US Army [16,17]. It was a third harmonic system. In that system, three experimental helicopter- and vehicle-mounted radars were developed to detect stationary military targets (tanks, vehicles, rifles and weapon caches) hidden by foliage. They successfully demonstrated a 1 km range capability by transmitting a 400 MHz signal (nominally) and receiving a 1200 MHz signal in return, i.e. the third harmonic. In recent times, the impetus is to have systems which exploit both the even and odd harmonics for detecting concealed weapons, electronics and other man-made objects [18].

The use of nonlinear radar to detect these interfaces is acknowledged to be difficult, because the effects depend strongly on the incident power and on range, and may be subject to false alarms from (for example) rusty metal objects or other metal-to-metal contacts. In particular, the target radar cross section is a function of the incident power density and of the harmonic number [14]. In addition, one has to be certain that the nonlinear effects are occurring in the target and not in the sensor. For such a radar system, the aim is to suppress linear returns from clutter while enhancing the nonlinear scattering from these components. As processing is based on *a priori* knowledge of the harmonics for filtering, pulses should be ideally sufficiently long to define the fundamental and hence higher harmonics, which limits range resolution. Moreover, if the incident pulse is shortened to improve range resolution, then its bandwidth increases, and the second harmonic generated by a nonlinear target response might not be at twice the centre frequency of the incident pulse (the frequency band in which the receiver is looking), but instead at twice the frequency of some resonance in the target that lies within the bandwidth of the incident pulse. Another limitation of harmonic radar is that the signal-to-noise ratio (SNR) can be low, because the bulk of the received echo energy remains at the fundamental and is filtered out.

A successful TWIPR device would potentially allow for the identification of semiconductor junctions, using the second- and higher-order even harmonics to distinguish them from linear scatterers and rusty metal. TWIPR is not limited as severely as harmonic radar because it works with an arbitrary waveform (constrained by reverberation and relative motion of source and receiver, not by the need to define a given fundamental frequency). Harmonic radar uses narrow bandwidths to prevent overlap between fundamental and harmonic components. The use in TWIPR of two pulses to interrogate the nonlinearity means that the incident waveform can have very great bandwidth, enhancing resolution and sensitivity, and opening up the opportunity of exciting nonlinearities from one or more resonances that are characteristic of the target but not known *a priori*.

The power of TWIPR's two-pulse system comes as much from the similarity of the pulses as their difference. The well-defined difference drives nonlinear systems in slightly different ways to generate large differences in responses. But just as importantly, the similarities between the two pulses allow the linear scattering to be reduced to zero using certain predictable combinations of the echoes. When these zeros are produced, high contrast, and easy distinction between linear and nonlinear scatterers is the result. An important feature that allows this is the similarity in terms of the spectral content of the two pulses.

Gaussian pulses are used in this particular study, although the principle was shown to work using BiaPSS for a range of other pulses, including a linear frequency-modulated pulse and dolphin-like clicks [6]. These could be of greater use if, for example, the resonance frequencies of components were not well known before the test, or if a particular target possessed several resonances that were to be used to identify it.

In TWIPR, as in TWIPS, the source emits a radiation time series, in which a pulse, $\psi_1(t)$, of duration T , is followed by a second similar pulse, $\psi_2(t)$, an interpulse time τ later. The variation between the first and second pulses will, in producing the echoes, be modified differently between various scatterers, depending on the form of the nonlinearity involved in the scattering process. Let the pulses be related by a relationship of the form $\psi_2(t) = \Gamma \psi_1(t)$, where Γ is a scalar. The

difference in amplitude will mean that two echoes from a linear scatterer only differ by the scaling factor Γ , whereas echoes from a nonlinear scatterer will not be related in that simple manner [6,7]. The efficacy of a general form of Γ is yet to be experimentally tested for radar, and TWIPR exploits the particular case of $\Gamma = -1$. That is to say, the second pulse is identical to the first, but with reversed polarity. The pulse pair can be expressed as $\Psi(t) = \psi_1(t) - \psi_1(t - \tau)$. In practical terms, the duration (T) and delay (τ) must be chosen, such that the reflections of the two pulses do not overlap. A linearly scattering target, for example soil, generates an echo $y_1(t)$ of the first pulse that can be described as a convolution of the incident pulse and the target's impulse response function, $h(t)$. This impulse response models the two-way propagation from source to target and the target's scattering characteristics. If a linearly scattering object is illuminated by the signal $\Psi(t)$, then the signal detected by the receiver is $y(t) = y_1(t) + y_2(t - \tau)$ in which $y_k(t)$ (where $k = 1, 2$) represents the convolution of the incident pulse and the impulse response function, specifically $y_k(t) = h(t) * \psi_k(t) = \int h(t - t')\psi_k(t') dt'$. Given that $\psi_2(t)$ differs from $\psi_1(t)$ by a factor Γ , then the response $y_2(t)$ is given by $y_2(t) = h(t) * \psi_2(t) = \Gamma y_1(t)$. Assume that the detection system uses a matched filter [19] that is scaled such that its overall gain is unity. In such circumstances, if the outputs of the matched filter for $y_k(t)$ are denoted $Y_k(t)$, where $k = 1, 2$, then it follows that $Y_2(t) = \Gamma Y_1(t)$. In the case of TWIPR, because $\Gamma = -1$ the addition of the reflections of the two pulses, to form a time history from the linear scatterer, produces zero (i.e. $Y_1(t) + Y_2(t) = 0$). The envelope of the summed signals is smoothed to form P_+ . The subtraction of the second echo from the first produces a signal with doubled amplitude (i.e. $Y_1(t) - Y_2(t) = 2Y_1(t)$), the smoothed amplitude of which is denoted P_- . The same pattern of suppression on addition and enhancement on subtraction occurs for odd-powered scattering whenever P_+ and P_- are formed. However, the contributions to the reflections that are produced by even powered scattering follow the opposite trend, being enhanced when P_+ is formed and suppressed in the signal P_- . This applies not just to the steady-state linear scatter, but also to linear scatter associated with ring-up [20] and ring-down [21]. Because the trends in suppression and enhancement are opposite for odd (including fundamental) harmonics and even ones, then, for example, comparison of the amplitudes of scattering structures in images of P_+ and P_- for the same field of view allows identification of linear scatterers from nonlinear ones and further distinction between those which scatter particular (e.g. odd or even) harmonics from those which do not. Signals formed from the ratios of these temporally averaged envelopes (i.e. P_-/P_+ and P_+/P_-) have the additional advantage of needing no time varying gain because automatic account is taken of the loss of amplitude with range [2,4,5,22–25]. Filters can also be used to enhance particular harmonics. The function P_{1-} is the end-product of a three-stage process, specifically: (i) subtracting the echo of the second pulse from that of the first, then (ii) applying a band filter (that has the same centre frequency as that of the incident pulses) to the result and then (iii) taking the temporal average of the envelope of the resulting signal over the duration (T) of the pulse. In similar vein, P_{2+} is obtained by: (i) adding the echo of the first pulse to that of the second, then (ii) applying a band filter (that has a centre frequency which is twice the centre frequency of the incident pulses) to the result, and then (iii) taking the temporal average of the envelope of the resulting signal over the duration (T) of the pulse.

A simple schematic showing how a TWIPR classifier might work is shown in figure 1. Assume that the excitation is sufficiently strong to excite up to the cubic nonlinearity. A pair of pulses, identical but with the second inverted with respect to the first, is projected at a field of view containing (i) soil/vegetation, (ii) semiconductor and (iii) rusty metal (figure 1*a*). The two pulses can be represented by the numbers '+1' and '-1', respectively. (In the simplified scheme shown in figure 1, the scattering of the nonlinearly scattering targets is represented only by squaring or cubing this digital representation of the incoming radar pulse, which greatly simplifies the process, but allows a more intuitive understanding (compared with the derivation of $Y_1(t) + Y_2(t) = 0$ and $Y_1(t) - Y_2(t) = 2Y_1(t)$, above) of the different effects of addition and subtraction of consecutive echoes if their scatterers are linear or exhibit differing nonlinear characteristics.)

The echoes of the two pulses from each of the target types in the field of view contain different sets of harmonics (figure 1*b*). Adding the two pulses in the echo (figure 1*c*) suppresses energy at

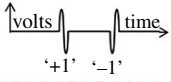
(a) twin inverted pulsed irradiate:	soil/vegetation	semiconductor	rusty metal
			
(b) echo contains energy at:	fundamental	all harmonics	odd harmonics
(c) add the two pulses of the echo:	$1 + (-1) = 0$ (suppressed) weak in P_{1+} weak in P_{2+} weak in P_{3+}	$1 + (-1) = 0$ (suppressed) $1^2 + (-1)^2 = 2$ (enhanced) $1^3 + (-1)^3 = 0$ (suppressed) weak in P_{1+} strong in P_{2+} weak in P_{3+}	$1 + (-1) = 0$ (suppressed) $1^3 + (-1)^3 = 0$ (suppressed) weak in P_{1+} weak in P_{2+} weak in P_{3+}
(d) subtract the two pulses of the echo:	$1 - (-1) = 2$ (enhanced) strong in P_{1-} weak in P_{2-} weak in P_{3-}	$1 - (-1) = 2$ (enhanced) $1^2 - (-1)^2 = 0$ (suppressed) $1^3 - (-1)^3 = 2$ (enhanced) strong in P_{1-} weak in P_{2-} strong in P_{3-}	$1 - (-1) = 2$ (enhanced) $1^3 - (-1)^3 = 2$ (enhanced) strong in P_{1-} weak in P_{2-} strong in P_{3-}
	(i)	(ii)	(iii)

Figure 1. Schematic of the expected characteristics for using TWIPR to distinguish between linear scatterers (here exemplified by soil and vegetation), semiconductors and rusty metal. (Online version in colour.)

odd (including linear) harmonics. The only enhancement it makes is for the semiconductor's even harmonics (figure 1c(ii)). By contrast, subtraction of the two pulses in the echo (figure 1d) enhances energy at odd (including linear) harmonics, and suppresses the semiconductor's even harmonics (figure 1d(ii)). The semiconductor is uniquely identified by P_{2+} as it is the only strong scatterer for that signal (identified by the black box in figure 1c(ii)). The soil can be distinguished from the other scatterers as it is the only item that is weak in P_{3-} , assuming for this simple scheme that there is sufficient SNR at such frequencies. This illustrative plot will need amending for a particular experiment when it is known how strongly the source signal used can excite particular nonlinearities. In the experiments conducted in this paper, the receiver system can detect the fundamental and second harmonic but not the third harmonic.

This method is now tested on scattering from a range of test objects. A simple experimental system with a fundamental and second harmonic receiver system will be used to demonstrate the efficacy of TWIPR on several test targets. A target of interest (representing semiconductors) is constructed from a dipole with a diode across its feedpoint. This is typical of covert circuitry one might wish to detect, and then (from its nonlinear scattering) distinguish from other metal, here represented by an aluminium plate (a linear scatterer) and a rusty bench clamp (a potentially nonlinear scatterer). In addition, two models of mobile phones are tested to see whether TWIPR can distinguish whether each is off, on or whether it contains a valid SIM card.

2. Method

A video of a TWIPR experiment is given in the electronic supplementary material. An arbitrary waveform generator (AWG), Tektronix AWG 7122B, produced a Gaussian-windowed sine wave pulse (figure 2a) consisting of 25 cycles centred on a 2.05 GHz carrier frequency. The duration (T) of each pulse was 12 ns, corresponding to a range resolution of around 1.8 m. The spectral

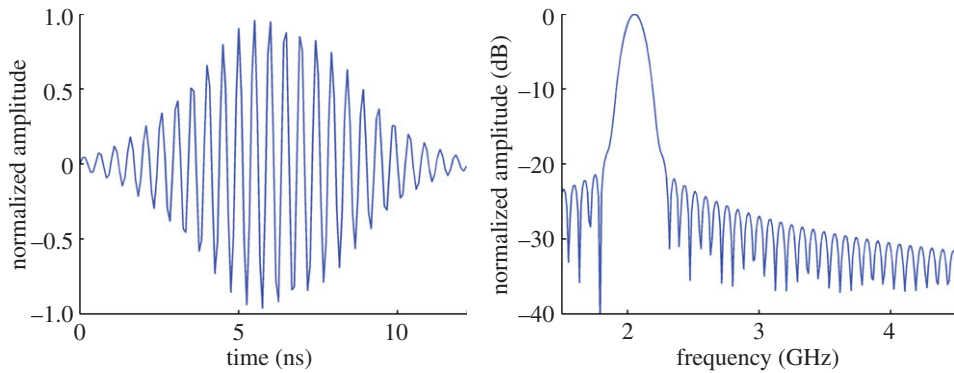


Figure 2. (a) Time history of one pulse in the pair, showing the normalized amplitude of the Gaussian-modulated waveform used. (b) The normalized amplitude (in dB) of the waveform used in frequency domain. The measured power referenced to 1 mW measured at 1.19 m is 39.7 dBm. (Online version in colour.)

width of each pulse (which is inversely proportional to the number of cycles) was here kept narrow (figure 2b), to ensure that the expected weaker signals (in the harmonics) from the nonlinear target would not be masked by the decaying side lobes of the transmit pulse in the frequency domain. A pulse repetition rate of 1 MHz was used to prevent overlapping of the return signals from two consecutive pulses.

The transmit pulses from the AWG are amplified using a Microwave Amps AM81 high-power amplifier (HPA), and then low-pass filtered before being radiated from the antenna (figure 3). The purpose of the low-pass filter was to attenuate the harmonics that were inevitably generated in the HPA (and would degrade the performance of TWIPR; [4]). In practice, the attenuation of harmonics could be optimized by adjusting the centre frequency and the bandwidth of the impulse so that the frequency of the second harmonic coincided with a null in the response of the low-pass filter or by preconditioning the drive pulse. Optimization is important as there is a trade-off set by the drive level between the generation of harmonics in the HPA and the peak power of the fundamental (which must be high to generate nonlinearities when scattered off the targets). The chosen components (e.g. low-pass filter and transmit antenna) had to be able to withstand the approximate 100 W rms operating power. In the receiver system, the fundamental of the signals is obtained directly from the cavity antenna, whereas the signals are high-pass filtered to improve the dynamic range of the system in the second harmonic. From the signals received, the TWIPR functions P_{1-} and P_{2+} can be analysed: the effectiveness of TWIPR relies on comparison of P_{1-} and P_{2+} , because analysis of P_{2+} alone is blind to the polarity of the incident pulse. Therefore, while it can enhance detection of nonlinear targets, the calculation of P_{1-} from the same echoes both enhances its ability to classify targets and can be used to obviate the need for time varying gain [4].

The measurements were taken in the anechoic chamber at University College London (UCL), which has an electromagnetic isolation of -110 dB from 1 to 40 GHz (figure 4a). The attenuations of the two types of absorbers in the chamber at normal incidence were less: -40 and -45 dB at 2 GHz. This anechoic chamber gave a controlled environment free of any measurable external interfering signals, and correspondingly, ensured that the experimental system did not cause interference to any external systems. The separation between the two antennas (the horn antenna and one octave receiver antenna; figure 4a) was 1.3 m with absorbers placed in between to reduce cross-beam interference.

Several targets have been used for the measurements. The ‘target of interest’ was a half-wavelength dipole which resonated at 2 GHz and whose input terminals were connected to a BAT54 Schottky diode (dipole + diode target; figure 4b). Clutter was represented by a piece of 1 mm thick aluminium plate with area 34×40 cm², irradiated broadside on and mounted on an

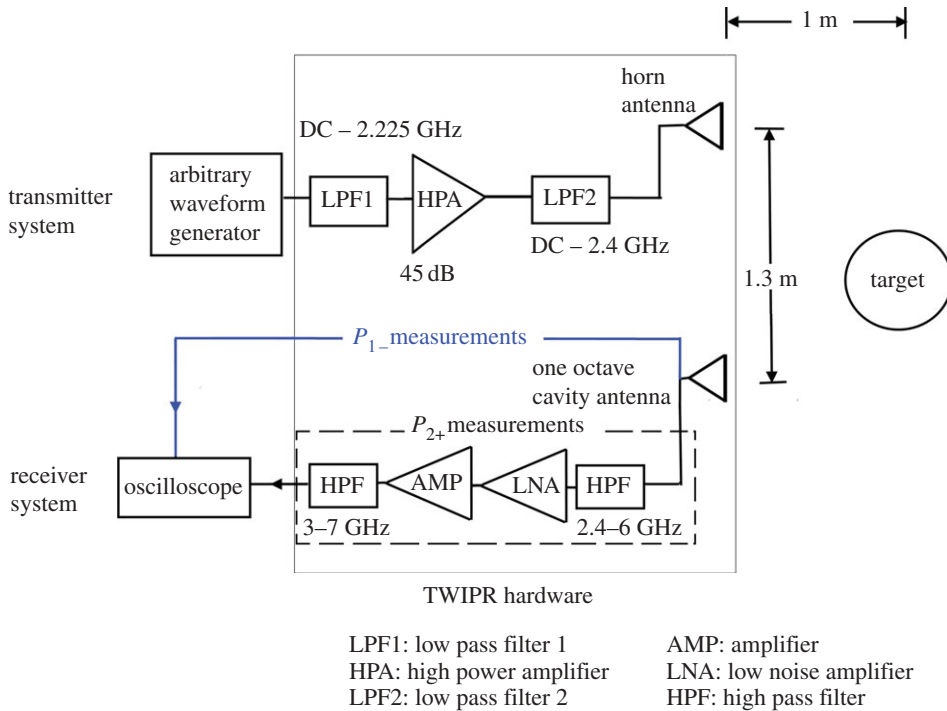


Figure 3. Block diagram of the experimental hardware.

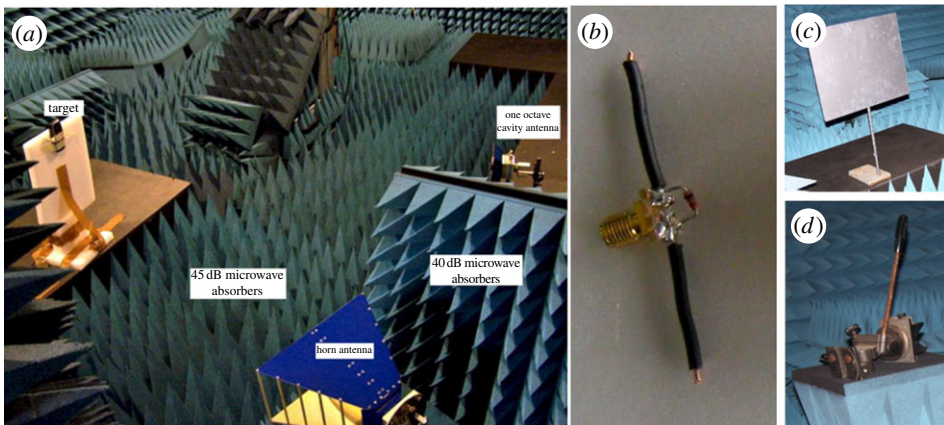


Figure 4. (a) The general experimental layout and the targets: (b) a BAT54 Schottky diode (dipole + diode target), which measure 6.3 cm tip-to-tip; (c) a piece of 1 mm-thick aluminium plate, with area $34 \times 40 \text{ cm}^2$ broadside onto the incident beam, mounted on an iron stand; and (d) a rusty bench clamp. One of the mobile phones can be seen in the target position in figure 4a.

iron stand (figure 4c). Other clutter was provided by a rusty bench clamp (figure 4d). Two mobile phones of different models (Nokia models N3330 and N3510, one of which can be seen in the target position in figure 4a) were tested in three states: turned on, turned off and turned on but with an invalid SIM card.

To excite nonlinearities, the incident radar pulse should be of high amplitude at the target, which required here that the transmitter be driven at its maximum capacity and that the target be as close as possible to the source. The targets were located at approximately 1 m from the

radar, where the rms power density incident on the target is 9.4 W m^{-2} . The data were acquired using a Tektronix DPO 72004 Digital Phosphor oscilloscope to perform the TWIPR tests (§3). The behaviours of the difference and sum TWIPR functions, P_{1-} and P_{2+} respectively, are obtained as described in §1 and are compared for the different targets. From the qualitative difference in form between the time domain envelopes of the TWIPR functions, P_{1-} and P_{2+} , the degree of nonlinearity in the reflections from the various targets is investigated for potential classification purposes.

3. Results

The TWIPR processing of the signals was undertaken on the time-series data obtained using the oscilloscope (the same normalization constant is used for all plots of P_{1-} data, and the same used for all P_{2+} data). Figure 5a shows the scattering response of the background conditions at the fundamental, P_{1-} , whereas figure 5b shows that of the TWIPR function, P_{2+} . The background conditions consist of the reflection of the foam block which is used to support the targets with the exception of the aluminium plate (figure 4a). The reflection of the considerably bigger aluminium plate was found to exceed significantly that of the foam block. Figure 5c,d shows the TWIPR functions of the aluminium plate in the time domain. Both the amplitudes of P_{1-} (figure 5c) and P_{2+} (figure 5d) are higher than that of the background. However, it is noted that while the amplitude of P_{1-} is several orders of magnitude higher than that of the background conditions, the amplitude of P_{2+} is only three times higher than that of the background. This suggests that the aluminium is predominantly a linear target for the stated exposure conditions. This also suggests the possibility that the experimental set-up is not able to eliminate completely the harmonics in the receiver system which become more significant when the reflection is high as in the aluminium plate.

For the dipole + diode target, although the linear scatter of P_{1-} is barely larger than the background (figure 5e), the TWIPR function P_{2+} at the target position is shown to exceed that of the background by several orders of magnitude (figure 5f). This suggests that there is a significant quadratic nonlinearity in the reflections from this target. This is in contrast to what was observed in figure 5d with regard to the aluminium plate. TWIPR has indeed exploited the higher second harmonic energy from the dipole + diode target and used it to distinguish from the aluminium plate target. It is noted that with an appropriate receiver antenna and filtering, TWIPR could be used to detect odd-powered nonlinearities of order 3 and higher if there were sufficient power emitted in them. Figure 5g,h shows the qualitative difference in form between the time domain envelopes of the TWIPR functions P_{1-} and P_{2+} for another type of practical target: a rusty bench clamp. Like the aluminium plate, the TWIPR function P_{2+} at the target position is shown to be close to that of the background (figure 5b), whereas the amplitude of P_{1-} is much higher than that of the background conditions. This implies that the rusty bench clamp is also predominantly a linear scatterer up to the second harmonic (figure 1d(iii)), just as the aluminium plate was for the stated exposure conditions.

To illustrate the complexity generated by a practical target, and the possibility of exploiting these characteristics by TWIPR in classifying different targets, the time domain envelopes of P_{1-} and P_{2+} for the mobile phones of different models are used. In addition, each mobile is also operated at three different states: switched on (labelled as 'on' in figures 6–8); switched off (labelled as 'off' in figures 6–8) and switched on with an out-of-date SIM card inserted (labelled as 'simcard' in figures 6–8). Given that mobile phones might contain multiple resonances and are themselves active sources through their communications with their base stations, this is a look-see experiment rather than a comprehensive study.

In similar vein to figure 5, the plots in figures 6 and 7 show the separate P_{1-} and P_{2+} functions. Figure 8 shows the ratio P_{2+}/P_{1-} expressed in dB for the targets shown here (the ratio is obtained from the peak value of the two TWIPR functions). While use of the ratio negates the need to use time varying gain, ideally the ratio P_{2+}/P_{1-} should be calculated after locations of strong SNR (which might therefore be targets requiring classification) have been identified, and moreover

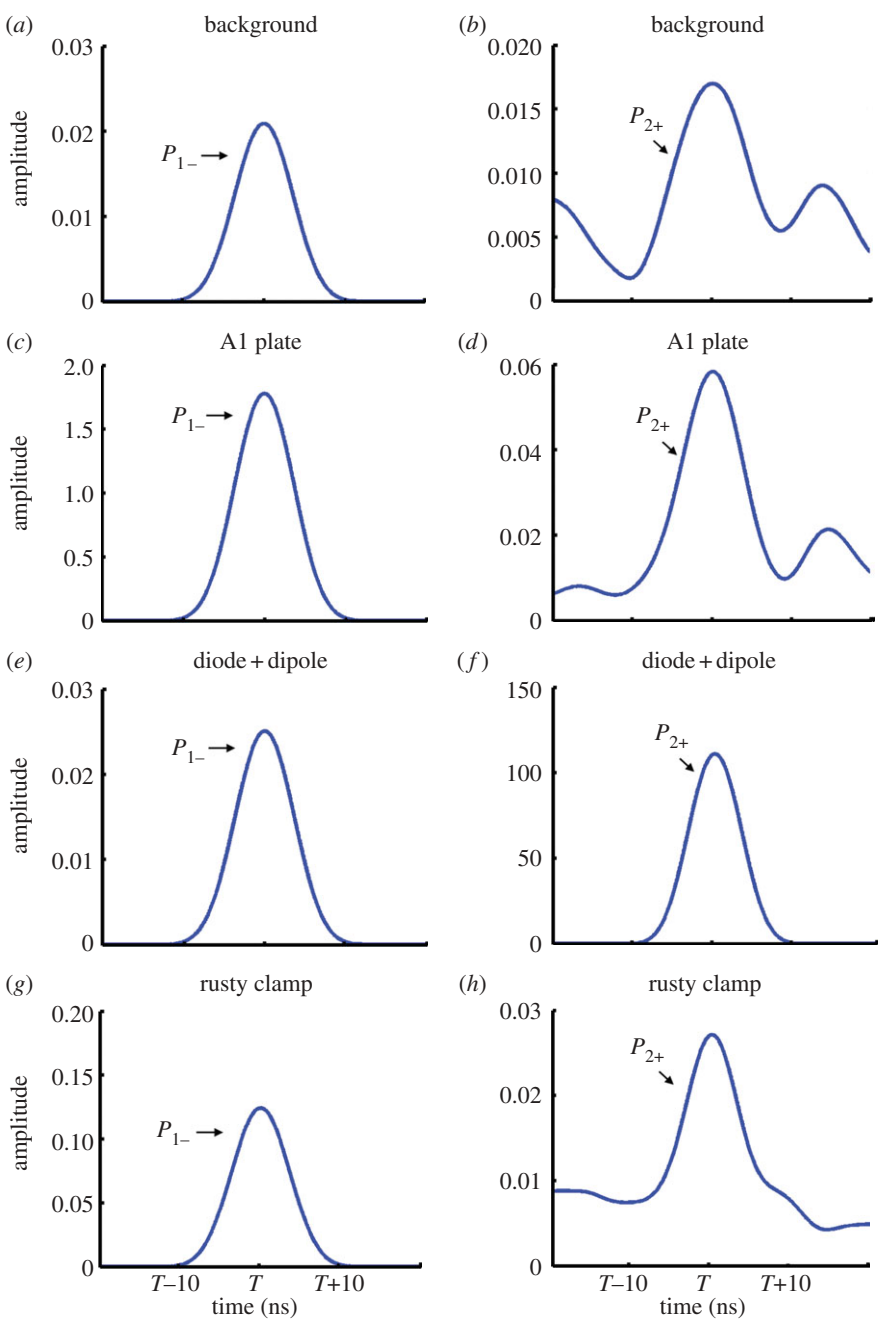


Figure 5. Measurements using TWIPR with the TWIPR functions P_{1-} and P_{2+} : (a) P_{1-} of background conditions, (b) P_{2+} of background conditions, (c) P_{1-} of aluminium plate, (d) P_{2+} of aluminium plate, (e) P_{1-} of diode + dipole target, (f) P_{2+} of diode + dipole target, (g) P_{1-} of rusty bench clamp and (h) P_{2+} of rusty bench clamp. The amplitudes of P_{1-} have been normalized by a value of 10^7 so as to obtain a meaningful comparison with P_{2+} . (Online version in colour.)

calculated only over the region of the location/time history where the possible targets are (i.e. where the SNR for either P_{1-} or P_{2+} is high). In regions away from such targets, the calculation of P_{2+}/P_{1-} can enhance the problems caused by noise, in particular when P_{1-} is very small and possibly dominated by noise.

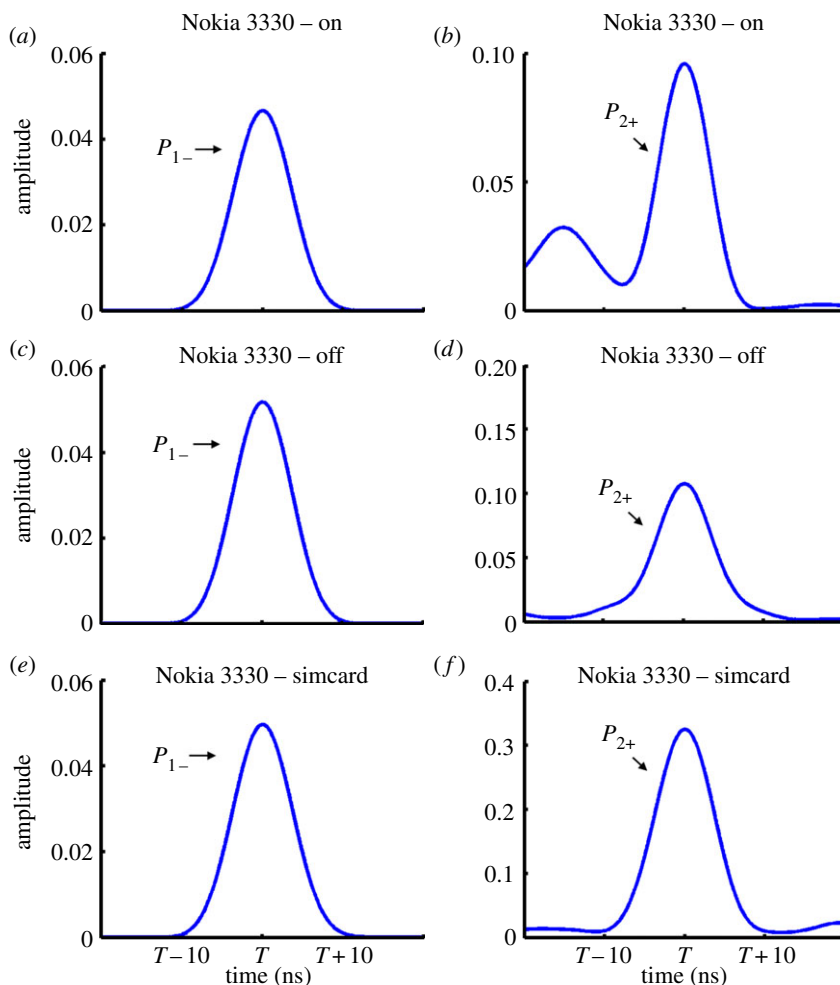


Figure 6. Measurements using TWIPR with the TWIPR functions P_{1-} and P_{2+} : (a) P_{1-} of Nokia 3330 (switched on), (b) P_{2+} of Nokia 3330 (switched on), (c) P_{1-} of Nokia 3330 (switched off), (d) P_{2+} of Nokia 3330 (switched off), (e) P_{1-} of Nokia 3330 (switched on with out-of-date SIM card inserted) and (f) P_{2+} of Nokia 3330 (switched on with out-of-date SIM card inserted). The amplitudes of P_{1-} have been normalized by a value of 10^7 so as to obtain a meaningful comparison with P_{2+} . (Online version in colour.)

For the set-up, the background condition (the scatter from the stand on which most targets are supported) gives a value of -0.9 dB. This provides the background colour away from the targets in figure 8. Having first normalized the amplitudes of P_{1-} by 10^7 , the colours for which $P_{2+}/P_{1-} < 1$ (the blues) indicate scattering that is detected as being predominantly linear (the receiver could only detect up to the quadratic nonlinearity). The colours for which $P_{2+}/P_{1-} > 1$ (the yellows, oranges and reds) indicate that the detected scattering is predominantly nonlinear. The dipole + diode ‘target of interest’, which from tip-to-tip measures 6.3 cm and weighs 2.8 g, is by far the strongest feature in figure 8. It is more than 28 dB stronger than the next most nonlinear item (the N3330 mobile phone with an invalid SIM card) and over 50 dB stronger than the 34×40 cm² aluminium plate that weighs 0.35 kg. For the various models of mobile phones, P_{2+}/P_{1-} is above 0 dB for Nokia 3330 in the three operating states tested, with the highest value of 8.2 dB obtained when an out-of-date SIM card is inserted with the mobile phone switched on. The Nokia 3510 is observed to behave mainly as a linear target when switched on with a valid SIM card, giving a low value of P_{2+}/P_{1-} (-11.1 dB). In the other operating states, it has a value close to

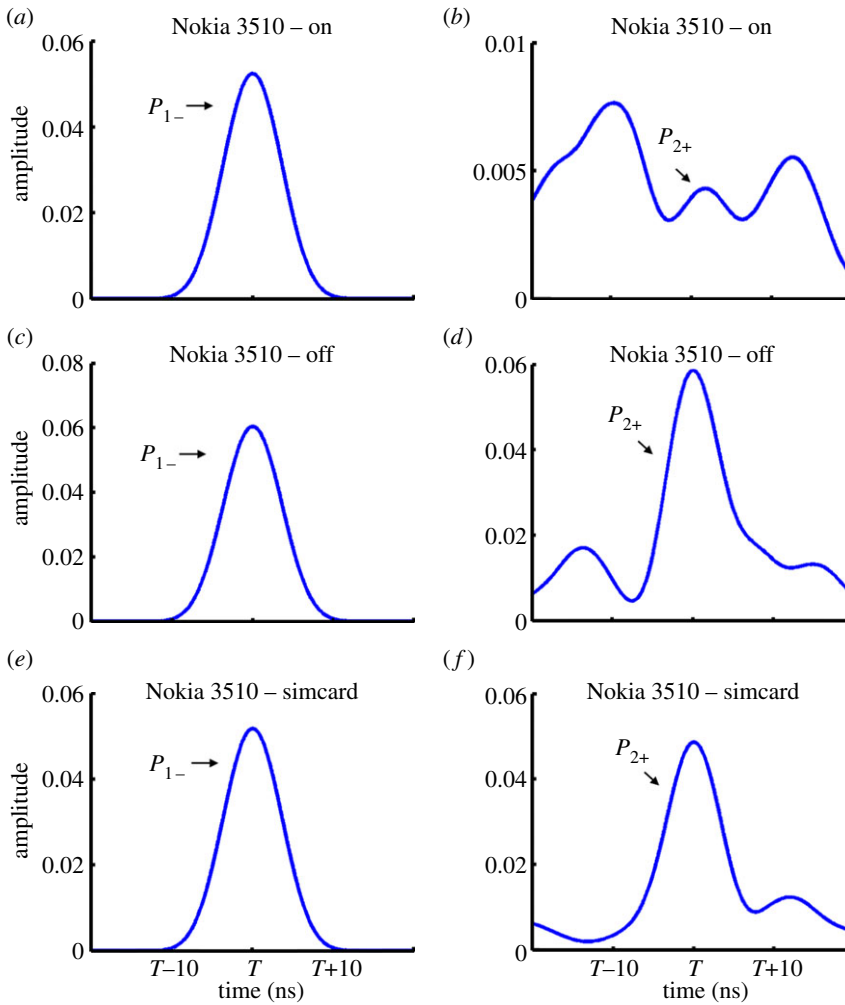


Figure 7. Measurements using TWIPR with the TWIPR functions P_{1-} and P_{2+} : (a) P_{1-} of Nokia 3510 (switched on), (b) P_{2+} of Nokia 3510 (switched on), (c) P_{1-} of Nokia 3510 (switched off), (d) P_{2+} of Nokia 3510 (switched off), (e) P_{1-} of Nokia 3510 (switched on with out-of-date SIM card inserted) and (f) P_{2+} of Nokia 3510 (switched on with out-of-date SIM card inserted). The amplitudes of P_{1-} have been normalized by a value of 10^7 so as to obtain a meaningful comparison with P_{2+} . (Online version in colour.)

background conditions, suggesting that it will be difficult to detect the mobile phone in these states using TWIPR with the pulses deployed here, because they were not designed to excite a specific phone resonance. Although both models of mobile phone are most linear for the pulses used here when switched on with a valid SIM card, this cannot be extrapolated to other models and frequencies without further tests. Recall that these phones are being tested with a narrowband TWIPR pulse and have unknown resonances. In summary, figure 8 shows that the values of the ratio of the TWIPR functions of the targets relative to the background conditions potentially can be used for classification purposes.

4. Conclusion

An experimental system, with the aim of demonstrating the efficacy of TWIPR for representative targets, was set up. TWIPR relies on the excitation of nonlinearities, which are favoured by high-amplitude pulses incident on a target. With the intensity of the highest amplitude pulses

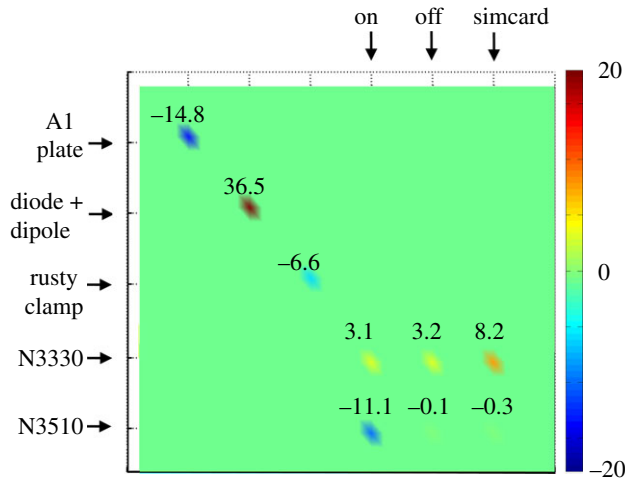


Figure 8. Colour map of the ratio P_{2+}/P_{1-} expressed in dB for the targets studied here. The dB value of the ratio for each target is denoted above the target position: note that the signal from the dipole + diode target is so strong that it exceeds the +20 dB full-scale deflection of the plot. The amplitudes of P_{1-} have been normalized by a value of 10^7 so as to obtain a meaningful comparison with P_{2+} .

achievable with the apparatus at 9.4 W m^{-2} rms, i.e. when the target was 1.19 m from the source, all the targets (an aluminium plate, a dipole + diode target, a rusty bench clamp and two different models of mobile phones) showed different degrees of nonlinearity in the output of the receiver.

Three representative targets were used to demonstrate the efficacy of TWIPR: an aluminium plate (to represent a linear scatterer) and a dipole + diode target (a nonlinear scatterer) and a rusty bench clamp. The TWIPR processing was able to distinguish what was the predominantly linear scatterer (the aluminium plate) from the nonlinear scatterer (the dipole + diode target). The scatter from a rusty bench clamp, which in principle can give nonlinear scatter in odd harmonics, was here predominantly linear because the receiver bandwidth could not acquire data at the third harmonic.

The possibility of using TWIPR on mobile phones was also demonstrated. By comparing the plots of the TWIPR functions, and using their ratios, the mobile phones and the other targets studied here were found to have varying degrees of nonlinearity in their reflections. Depending on the phone models, the degree of nonlinearity varied with the operating state when subjected to the narrowband pulse shown here. This suggests that there is a possibility that the differing operating states of a mobile phone can be distinguished using TWIPR, particularly if wideband pulses are used, although in practice this would be complementary to other data (a phone with a valid SIM card establishes a dialogue with a base station, so is emitting a signal that can intermodulate with an incident radar signal).

These preliminary tests demonstrate the efficacy of TWIPR in detecting nonlinearly scattering targets and distinguishing them from linear ones. These results suggest that other pulse processing schemes, for example BiaPSS [6], would potentially also be operable with radar and with other electromagnetic radiations (MRI, LIDAR [1,4]). For TWIPR to work, the amplitude of the pulse incident on the target must be sufficiently high. In many applications, this might suggest bistatic operation with remotely deployable sources, placing the source sufficiently close to the target to excite nonlinear scatter which is then detected remotely.

The diode + dipole target shown in figure 4b measures 6.3 cm in length, weighs 2.8 g, costs less than 1 Euro, is very simple to manufacture and requires no batteries. Given these features, and the fact that they can easily be tuned to scatter specific resonances to provide a unique identifier to

a broadband TWIPR pulse, they offer the possibility of tags for animals or autonomous vehicles hidden in foliage, underground or in infrastructure (pipelines, conduits, etc.); and for humans entering hazardous areas, particularly where they might be underground or buried. If a hazard is expected (for rescue workers, miners or climbers in avalanche areas), tags can be carried. The results of figure 8 suggest that, if tags are not carried, TWIPR can carry the bandwidth to search for mobile phone resonances, and so offer the possibility of locating victims by identifying the TWIPR scatter from their mobile phones (e.g. in collapsed buildings), even when the phones are turned off or the batteries have no charge remaining.

Acknowledgements. G.H.C.'s PhD was undertaken while he was on a full-time scholarship from DSO National Laboratories, Singapore. For associated movies, interested readers are directed to <http://rspa.royalsocietypublishing.org/content/early/2012/07/17/rspa.2012.0247/suppl/DC1> for an explanation of the preceding sonar studies [4–6]. In addition, the supplementary material of this paper contains two movies, one of a sonar TWIPS experiment and the other of a TWIPR experiment.

References

1. Leighton TG, White PR, Finfer DC. 2008 Hypotheses regarding exploitation of bubble acoustics by cetaceans. In *Proc. 9th European Conf. on Underwater Acoustics (ECUA 2008)*, Paris, France, 29 June–4 July, pp. 77–82. Paris, France: SFA.
2. Leighton TG, White PR, Finfer DC. 2009 Contrast enhancement between linear and nonlinear scatterers. European Patent Application 06755621.7 and US Patent Application 11/917,990; from International patent application number PCT/GB2006/002335 (filed 26 June 2006).
3. Leighton TG. 2004 From seas to surgeries, from babbling brooks to baby scans: the acoustics of gas bubbles in liquids. *Int. J. Mod. Phys. B* **18**, 3267–3314. (doi:10.1142/S0217979204026494)
4. Leighton TG, Finfer DC, White PR, Chua GH, Dix JK. 2010 Clutter suppression and classification using twin inverted pulse sonar (TWIPS). *Proc. R. Soc. A* **466**, 3453–3478. (doi:10.1098/rspa.2010.0154)
5. Leighton TG, Finfer DC, Chua GH, White PR, Dix JK. 2011 Clutter suppression and classification using twin inverted pulse sonar in ship wakes. *J. Acoust. Soc. Am.* **130**, 3431–3437. (doi:10.1121/1.3626131)
6. Leighton TG, Chua GH, White PR. 2012 Do dolphins benefit from nonlinear mathematics when processing their sonar returns? *Proc. R. Soc. A* **468**, 3517–3532. (doi:10.1098/rspa.2012.0247)
7. Chua GH, White PR, Leighton TG. 2012 Use of clicks resembling those of the Atlantic bottlenose dolphin (*Tursiops truncatus*) to improve target discrimination in bubbly water with biased pulse summation sonar. *IET Radar, Sonar Navig.* **6**, 510–515. (doi:10.1049/iet-rsn.2011.0199)
8. Lui PL. 1990 Passive intermodulation interference in communication systems. *IEEE Electron. Commun. Eng.* **2**, 109–118. (doi:10.1049/ecej:19900029)
9. Burns PN, Wilson SR. 2006 Microbubble contrast for radiological imaging: 1. Principles. *Ultrasound Q.* **22**, 5–13.
10. Daniels DJ. 2009 *EM detection of concealed targets*. In Wiley Series in Microwave and Optical Engineering. Hoboken, NJ: John Wiley & Sons, Inc.
11. Colpitts BG, Boiteau G. 2004 Harmonic radar transceiver design: miniature tags for insect tracking. *IEEE Trans. Antennas Propag.* **52**, 2825–2832. (doi:10.1109/TAP.2004.835166)
12. Lovei GL, Stringer IAN, Devine CD, Cartellier M. 1997 Harmonic radar: a method using inexpensive tags to study invertebrate movement on land. *N. Z. J. Ecol.* **21**, 187–193.
13. Riley JR, Smith AD. 2002 Design consideration for an harmonic radar to investigate the flight of insects at low altitude. *Comput. Electron. Agric.* **35**, 151–169. (doi:10.1016/S0168-1699(02)00016-9)
14. Harger RO. 1976 Harmonic radar systems for near-ground in foliage nonlinear scatterers. *IEEE Trans. Antennas Propag.* **12**, 230–245.
15. Shteinshleiger VB. 1984 Nonlinear scattering of radio waves by metallic objects. *Soviet Phys. Usp.* **27**, 131–145. (doi:10.3367/UFNr.0142.198401e.0131)
16. Elsner RF. 1974 *Vehicular variable parameter METRRA system*. Chicago, IL: IIT Research Institute.

17. Dauben DA, Hull D. 1978 METRRA signature - radar cross section measurements. Final report/instruction manual. San Diego, CA: Cubic Corp Defense Systems Div.
18. Jablonski DG, Ko HW, Oursler DA, Smith DG, White DM. 2004 System and method of radar detection of non-linear interfaces. Patent no. US 6,765,527 B2. The Johns Hopkins University.
19. Burdic WS. 1984 *Underwater acoustic system analysis*. Prentice-Hall Signal Processing Series. Englewood Cliffs, NJ: Prentice-Hall, Inc.
20. Clarke JW, Leighton TG. 2000 A method for estimating time-dependent acoustic cross-sections of bubbles and bubble clouds prior to the steady state. *J. Acoust. Soc. Am.* **107**, 1922–1929. (doi:10.1121/1.428474)
21. Leighton TG, Meers SD, White PR. 2004 Propagation through nonlinear time-dependent bubble clouds and the estimation of bubble populations from measured acoustic characteristics. *Proc. R. Soc. Lond. A* **460**, 2521–2550. (doi:10.1098/rspa.2004.1298)
22. Leighton TG, White PR, Finfer DC. 2005 Target detection in bubbly water. British Patent Application no. 0513031.5. University of Southampton.
23. Tang M-X, Mari J-M, Wells PNT, Eckersley RJ. 2008 Attenuation correction in ultrasound contrast agent imaging: elementary theory and preliminary experimental evaluation. *Ultrasound Med. Biol.* **34**, 1998–2008. (doi:10.1016/j.ultrasmedbio.2008.04.008)
24. Leighton TG, Finfer DC, White PR. 2009 Two hypotheses about cetacean acoustics in bubbly water (bio-acoustics 2009). *Proc. Inst. Acoust.* **31**, 119–128.
25. Leighton TG, White PR, Finfer DC. 2009 Hypotheses on the acoustics of whales, dolphins and porpoises in bubbly water. In *Proc. 3rd Int. Conf. on Underwater Acoustic Measurements, Technologies and Results* (eds JS Papadakis, L Bjorno), Nafplion, Greece, 21–16 June, pp. 3–14. Heraklion, Crete, Greece: IACM-FORTH.